Residential and Race/Ethnicity Disparities in Heat Vulnerability in the United States

Mitchell Manware[1,2], Robert Dubrow[2,3], Daniel Carrión[2,3], Yiqun Ma[2,3] , and Kai Chen[2,3]

[1]Department of Social and Behavioral Sciences, Yale School of Public Health, New Haven, CT, USA, [2]Yale Center on Climate Change and Health, Yale School of Public Health, New Haven, CT, USA, [3]Department of Environmental Health Sciences, Yale School of Public Health, New Haven, CT, USA

Abstract Adverse health outcomes caused by extreme heat represent the most direct human health threat associated with the warming of the Earth's climate. Socioeconomic, demographic, health, land cover, and temperature determinants contribute to heat vulnerability; however, nationwide patterns of residential and race/ethnicity disparities in heat vulnerability in the United States are poorly understood. This study aimed to develop a Heat Vulnerability Index (HVI) for the United States; to assess differences in heat vulnerability across geographies that have experienced historical and/or contemporary forms of marginalization; and to quantify HVI by race/ethnicity. Principal component analysis was used to calculate census tract level HVI scores based on the 2019 population characteristics of the United States. Differences in HVI scores were analyzed across the Home Owners' Loan Corporation (HOLC) "redlining" grades, the Climate and Economic Justice Screening Tool (CEJST) disadvantaged versus non-disadvantaged communities, and race/ethnicity groups. HVI scores were calculated for 55,267 U.S. census tracts. Mean HVI scores were 17.56, 18.61, 19.45, and 19.93 for HOLC grades "A"–"D," respectively. CEJST-defined disadvantaged census tracts had a significantly higher mean HVI score (19.13) than non-disadvantaged tracts (16.68). The non-Hispanic African American or Black race/ethnicity group had the highest HVI score (18.51), followed by Hispanic or Latino (18.19). Historically redlined and contemporary CEJST disadvantaged census tracts and communities of color were found to be associated with increased vulnerability to heat. These findings can help promote equitable climate change adaptation policies by informing policymakers about the national distribution of place- and race/ethnicity-based disparities in heat vulnerability.

Plain Language Summary As the Earth's climate warms, extreme heat is the most direct threat to human health. Due to various socioeconomic, demographic, health, and environmental factors, some individuals and populations are more vulnerable to adverse health events caused by extreme heat. Publicly available data were obtained for each of these factors, and statistical analysis yielded a quantitative measure of heat vulnerability for 55,267 U.S. census tracts. Of these census tracts, those that have experienced historical and/or contemporary forms of marginalization were associated with increased vulnerability to heat. Additionally, non-White race/ethnicity groups were associated with increased vulnerability to heat and were overrepresented in the census tracts with the highest vulnerability. These results can inform policymakers of the places and race/ethnicity groups most vulnerable to heat, and can therefore be used to develop equity-promoting climate change adaptation policies.

1. Introduction

Adverse health outcomes associated with extreme heat represent the most direct human health threat of the warming of the Earth's climate caused by anthropogenic greenhouse gas emissions (Z. Xu et al., 2016; Zhai et al., 2021). Disparities in heat exposure, exacerbated by disparities in access to individual- and community-level protective factors, result in inequitable distribution of the burden of heat-related illness across geographic locations, occupations, and demographic characteristics (Campbell et al., 2018). The disproportionate exposure of communities of color in the United States to environmental hazards, often ascribed at least in part to racially driven residential segregation policies, is a fundamental manifestation of environmental racism (Bravo et al., 2016; Chavis, 1994; Gee & Payne-Sturges, 2004; Lopez, 2002; Morello-Frosch & Jesdale, 2006; Perry, 2007). Recently, heat-related outpatient emergency department visits and inpatient admissions from the emergency department were found to be higher in "redlined" neighborhoods, evidence of the potential adverse health consequences at the intersection of racist policies and climate change (Li et al., 2021).

Investigation: Mitchell Manware, Kai Chen
Methodology: Mitchell Manware, Robert Dubrow, Daniel Carrión, Kai Chen
Resources: Mitchell Manware, Kai Chen
Supervision: Kai Chen
Visualization: Yiqun Ma
Writing – original draft: Mitchell Manware
Writing – review & editing: Robert Dubrow, Daniel Carrión, Yiqun Ma, Kai Chen

The term "redlining" stems from lending maps created by the Home Owners' Loan Corporation (HOLC) in the 1930s (Pearcy, 2020). Across urban areas in the United States, maps were created to assess a neighborhood's level of loan risk based on its physical building conditions, public utilities and, infamously, demographic composition (Pearcy, 2020). Neighborhoods with African American, Hispanic, Asian, and Jewish populations were often graded the lowest, resulting in denied mortgage loans and limited wealth accumulation among these communities (Aaronson et al., 2021; Pearcy, 2020). City-wide maps displaying neighborhood grades were color coded, with the highest-risk areas colored red, giving rise to the term "redlining" (Pearcy, 2020). Recently, the White House Council on Environmental Quality created the Climate and Economic Justice Screening Tool (CEJST), which identifies "disadvantaged" communities based on various socioeconomic, environmental, and health criteria (Climate and Economic Justice Screening Tool, 2022a, 2022b). The CEJST provides a contemporary measure of residential disparity in the United States, though differing from HOLC grades by its inclusion of suburban and rural areas, as well as by its equity promoting purpose (Climate and Economic Justice Screening Tool, 2022a, 2022b).

HOLC "redlining" grades and CEJST advantage status provide unique, insightful measures of residential disparity, each supporting environmental justice research by capturing a range of place-based exposures and outcomes (Smoyer, 1998). Previous studies have observed higher land surface temperature (LST), less green space, and more dark roofs in "redlined" census tracts (Hoffman et al., 2020; Namin et al., 2020; Nardone et al., 2021; Schinasi et al., 2022; Wilson, 2020). However, these studies did not assess the association between HOLC grade and various socioeconomic, demographic, or biological determinants of heat vulnerability (World Health Organization, 2021), nor did they analyze potential differences in heat vulnerability by race/ethnicity. Furthermore, previous heat vulnerability indices have been developed for individual cities (Conlon et al., 2020; Johnson et al., 2012; Mallen et al., 2019; Wolf & McGregor, 2013), counties (Harlan et al., 2013; Prudent et al., 2016), or states (Maier et al., 2014; Nayak et al., 2018), and the only national Heat Vulnerability Index (HVI) was limited by missing data and lack of a heat exposure variable (Reid et al., 2009).

To fill these gaps, we aimed to better understand place-based and race/ethnicity-based disparities in heat vulnerability across the entire United States. We build on the aforementioned research by (a) developing an expansive and uniform HVI for the contiguous United States; (b) assessing how the HVI differs across historical (i.e., HOLC grade) and contemporary (i.e., CEJST) measures of residential disparity; and (c) quantifying the HVI distribution by race/ethnicity. We hypothesized that heat vulnerability would be greatest in both historically defined and contemporaneously defined disadvantaged communities and in communities of color.

2. Methods

2.1. Data Sources

2.1.1. Heat Vulnerability Index (HVI) Data

We evaluated the peer-reviewed literature to identify candidate variables for the HVI, (i.e., variables found to be associated with heat-related adverse health outcomes, Table 1). Of the variables with supporting evidence, only those with nationwide data available at the county or census tract levels were included. Data used to construct the HVI included demographic, economic, social, housing, diabetes, land cover, and temperature variables collected from various sources (Table 2). All data points were collected at or calculated to the census tract level. We obtained complete data for 55,267 census tracks, with 18,735 census tracts excluded from the HVI analysis due to missing data for one or more variables.

Demographic, economic, social, and housing data was obtained at the census tract level from various American Community Survey (ACS) 5-Year Estimates from 2019. Demographic data consisted of the Hispanic or Latino, non-Hispanic African American or Black, and elderly population proportions of each census tract (ACS Demographic and Housing Estimates, 2019). Economic data included the proportion of unemployed individuals and individuals living below the federal poverty level (Poverty Status in the Past 12 Months, 2019; Selected Economic Characteristics, 2019). Social variables included the proportions of individuals living alone, elderly and living alone, disabled, with less than a high school education, born in a foreign country, and who are limited English proficient (Selected Social Characteristics in the United States, 2019). The proportion of homes built prior to 1980 constituted the housing data (Physical Housing Characteristics for Occupied Housing Units, 2019).

Table 1
Heat Vulnerability Index Variables and Supporting Literature[a]

Variable	Supporting literature
Percentage population that is Hispanic or Latino	Uejio et al. (2011), Knowlton et al. (2009), Jones et al. (1982), and Lin et al. (2009)
Percentage population that is non-Hispanic African American or Black	Uejio et al. (2011), Schwartz (2005), Whitman et al. (1997), Jones et al. (1982), O'Neill et al. (2005), O'Neill et al. (2003), and Zanobetti et al. (2013)
Percentage population that is elderly	Gronlund et al. (2016), Semenza et al. (1999), Anderson and Bell (2009), Jones et al. (1982), and Whitman et al. (1997)
Percentage population that is unemployed	Anderson and Bell (2009) and Hansen et al. (2013)
Percentage population living below the federal poverty level	Curriero et al. (2002), Naughton et al. (2002), Jones et al. (1982), and Zanobetti et al. (2013)
Percentage population that is living alone	Naughton et al. (2002), Semenza et al. (1996), and Uejio et al. (2011)
Percentage population that is elderly and living alone	Gronlund et al. (2016), Semenza et al. (1999), Anderson and Bell (2009), Jones et al. (1982), Whitman et al. (1997), Naughton et al. (2002), Semenza et al. (1996), and Uejio et al. (2011)
Percentage population that is disabled	N. Bark (1998), N. M. Bark (1982), and Kaiser et al. (2001)
Percentage population with less than a high school education	Curriero et al. (2002), Zanobetti et al. (2013), and O'Neill et al. (2003)
Percentage population that was born in a foreign country	Chow et al. (2012)
Percentage population that is limited English proficient	Uejio et al. (2011), McGeehin and Mirabelli (2001), and Hansen et al. (2013)
Percentage of occupied houses built before 1980	Gronlund et al. (2015) and Y. Xu et al. (2013)
Percentage of adults age 20+ diagnosed with diabetes	Semenza et al. (1999), Semenza et al. (1996), Schwartz (2005), and Knowlton et al. (2009)
Percentage of land covered in high density development	Uejio et al. (2011), Jones et al. (1982), Harlan et al. (2006), Clarke (1972), and Buechley et al. (1972)
Percentage of land covered in non-green space	Gronlund et al. (2015), Zanobetti et al. (2013), Kilbourne et al. (1982), Y. Xu et al. (2013), Harlan et al. (2006), and Harlan et al. (2013)
Average summertime enhanced vegetation index (EVI) score	Gronlund et al. (2015), Harlan et al. (2006), and Harlan et al. (2013)
Average summertime 2m air temperature anomaly (°F)	Harlan et al. (2006), Johnson and Wilson (2009), Avashia et al. (2021), Basu et al. (2008), Medina-Ramón and Schwartz (2007), and Zanobetti and Schwartz (2008)

[a]Supporting literature identifies research studies that support a relationship between the given variables and adverse heat-related health outcomes.

Diabetes prevalence was used to represent underlying health conditions based on the association between diabetes and heat-related adverse health outcomes (Knowlton et al., 2009; Schwartz, 2005; Semenza et al., 1996, 1999), the co-prevalence of diabetes with several other comorbid conditions (Iglay et al., 2016), and the availability of nationwide diabetes prevalence data (United States Diabetes Surveillance System, 2021). Sex-specific census-tract-level diabetes prevalence for persons aged 20 years and older was estimated using county-level diabetes data collected from the Center for Disease Control and Prevention (CDC) U.S. Diabetes Surveillance System and census-tract-level age and sex data collected from the ACS 5-Year Age and Sex Estimates (Age and Sex, 2019; United States Diabetes Surveillance System, 2021). Specifically, we used CDC sex-specific diabetes prevalence estimates for individuals aged 20 years and older for years 2015–2019 to calculate a 5-year, sex-specific estimate for each county. Then, we multiplied each sex- and county-specific prevalence estimate by the number of males and females aged 20 years and older, respectively, in each census tract within each county to estimate the total number of diabetic male and female individuals in each census tract. The sex-specific totals were summed and divided by the total population aged 20 years and older in each census tract to estimate the total 5-year average diabetes prevalence in each census tract.

We obtained two land cover variables—high density development and non-green space—from the National Neighborhood Data Archive (NaNDA): Land Cover by Census Tract, United States, 2001–2016 data file (Clarke & Melendez, 2019). High density development is an NaNDA-defined variable that measures the proportion of land within each census tract having urban imperviousness greater than 79% (Clarke & Melendez, 2019). The non-green space variable was calculated by summing the proportion of land within each census tract that was covered in "green space" (deciduous forest, evergreen forest, mixed forest, shrub/scrub, herbaceous, hay/pasture, cultivated crops, woody wetlands, and emergent herbaceous wetlands), subtracting from 1 and multiplying by

Table 2
Heat Vulnerability Index Data Sources and Descriptive Statistics

Category	Data source	Year range	Variable	Mean	SD	(Min, max)
Demographic variables	American Community Survey 5-Year demographic and housing estimates	2015–2019	Percentage population that is Hispanic or Latino	16.58	21.44	(0, 100)
		2015–2019	Percentage population that is non-Hispanic African American or Black	14.08	22.25	(0, 100)
		2015–2019	Percentage population that is elderly	16.54	7.91	(0, 92.2)
	American Community Survey 5-Year selected economic characteristics	2015–2019	Percentage population that is unemployed	3.54	2.49	(0, 100)
	American Community Survey 5-Year selected social characteristics	2015–2019	Percentage population that is living alone	28.23	11.26	(0, 100)
		2015–2019	Percentage population that is elderly and living alone	11.29	6.11	(0, 100)
		2015–2019	Percentage population that was born in a foreign country	12.58	13.59	(0, 100)
		2015–2019	Percentage population that is limited English proficient	7.88	10.69	(0, 100)
		2015–2019	Percentage population that is disabled	11.18	6.33	(0, 100)
		2015–2019	Percentage population with less than a high school education	12.76	10.35	(0, 100)
	American Community Survey 5-Year poverty status in the past 12 months	2015–2019	Percentage population living below the federal poverty level	14.75	11.59	(0, 100)
Housing variable	American Community Survey 5-Year physical housing characteristics for occupied Housing Unit	2015–2019	Percentage of occupied houses built before 1980	60.94	26.19	(0, 100)
Underlying health conditions variable	Centers for disease control and prevention. U.S. diabetes surveillance system website	2014–2018	Percentage of adults age 20+ diagnosed with diabetes	6.83	1.38	(0.99, 15.78)
	American Community Survey 5-Year age and sex	2015–2019				
Land cover variables	National Neighborhood Data Archive (NaNDA): Land cover by census tract, United States, 2001–2016	2016	Percentage of land covered in high density development	9.2	15.51	(0, 100)
		2016	Percentage of land covered in non-green space	64.89	36.66	(0.03, 100)
	MOD13A2 MODIS/terra vegetation indices 16-day L3 global 1 km SIN grid V006[a]	2017–2020	Average summertime enhanced vegetation index (EVI) score	0.37	0.14	(0, 0.68)
Exposure variable	Daymet: Daily surface weather data on a 1-km grid for North America, version 4	2017–2020	Average summertime 2m air temperature anomaly (°F)	2.97	6.09	(−4.51, 40.54)

[a]NASA's Terra and Aqua satellites' Moderate Resolution Imaging Spectroradiometer.

100 (Clarke & Melendez, 2019). This value represents the percentage of land in each census tract covered by non-natural, artificial surfaces (Clarke & Melendez, 2019).

A third land cover variable—an average enhanced vegetation index (EVI) score, which is an alternative measure of vegetation greenness—was calculated for each census tract using data downloaded from NASA's MOD13A2 Version 6 Product (Didan, 2015). A 4-year average of summer-month EVI scores was calculated using 16-day EVI scores from 1 June through 31 August for years 2017 through 2020 (Didan, 2015). One square kilometer grid cell layers representing each 16-day period within the date range were stacked to calculate the average EVI score for each grid cell (Didan, 2015). The average EVI values for each grid cell were aggregated to the census tract level by taking the area-weighted mean of each EVI score within the census tract polygon (Didan, 2015). This calculation yielded a census-tract-level average EVI score for the summer months from 2017 to 2020 (Didan, 2015). The EVI was preferred over the Normalized Difference Vegetation Index for its increased sensitivity over heavily vegetated areas and correction for both atmospheric conditions and canopy background (Nawrot et al., 2007; Qian et al., 2008).

Air temperature at 2-m height was obtained from NASA's Daymet Version 4 data set and used to measure heat exposure for each census tract (Thornton et al., 2020). A 4-year average of non-missing air temperatures was calculated for each 1 km^2 grid cell using air temperature data from 1 June through 31 August for years 2017 through 2020 (Thornton et al., 2020). Average grid cell air temperature was aggregated to the census tract level by taking the area-weighted mean of each air temperature value within the census tract polygon, yielding average 2-m air temperature for the summer months. Census tracts' most frequently occurring temperature (MFT) was calculated using air temperature at 2-m height data from 1 January 2000 through 31 December 2020, obtained from NASA's Daymet Version 4 data set (Thornton et al., 2020). Temperature estimates were rounded to the nearest degree, and the modal temperature estimate for each grid cell represented the MFT. Grid cell MFT estimates were aggregated to the census tract level by taking the area-weighted mean of each temperature estimate within the census tract polygon, yielding the 20-year MFT for each census tract. Heat exposure for each census tract was measured by calculating the difference between the average 2-m air temperature for the summer months and the 20-year MFT. Quantifying heat exposure based on recent summer months' temperature anomaly relative to the MFT captures spatial differences in summertime warming and potentially incorporates an aspect of local climate adaptation (Spangler & Wellenius, 2020).

2.1.2. Residential Disparity Data

HOLC data were obtained from the Inter-university Consortium for Political and Social Research's *Historic Redlining Scores for 2010 and 2020 US Census Tracts* project (Meier & Mitchell, 2021). This project overlaid HOLC maps with 2020 census tract polygons to calculate a weighted average HOLC score for recent census tract boundaries (Meier & Mitchell, 2021). HOLC grades ranged from "A" to "D," where "A" was "Best," "B" was "Desirable," "C" was "Definitely Declining," and "D" was "Hazardous" (Nelson et al., 2020; Pearcy, 2020). The original HOLC grades were converted to numbers for calculation purposes (A = 1, B = 2, C = 3, and D = 4) (Meier & Mitchell, 2021). The resulting census-tract-level-weighted HOLC scores for 2020 census tract boundaries ranged continuously from 1.0 to 4.0 and were available for 13,488 census tracts across 142 cities (Meier & Mitchell, 2021).

Disadvantaged community data were obtained from the White House Council on Environmental Quality's CEJST (Climate and Economic Justice Screening Tool, 2022a, 2022b). Data utilized for this analysis consisted of the tool's binary census-tract-specific disadvantage indicator ("disadvantaged" or "non-disadvantaged"), along with each census tract's unique geographic identifier (GEOID) (Climate and Economic Justice Screening Tool, 2022a, 2022b). The CEJST identifies a census tract as "disadvantaged" if it exceeds the threshold for one or more environmental or climate indicators and for both socioeconomic indicators within at least one of the tool's eight categories of criteria (Climate and Economic Justice Screening Tool, 2022a, 2022b).

Race and ethnicity population data were collected from ACS 5-Year Demographic and Housing Estimates from 2019 (ACS Demographic and Housing Estimates, 2019). Race and ethnicity were combined, producing eight groups for comparison: Hispanic or Latino of any race, non-Hispanic White, non-Hispanic Black or African American, non-Hispanic American Indian and Alaska Native, non-Hispanic Asian, non-Hispanic Native Hawaiian and Other Pacific Islander, non-Hispanic Other race, and non-Hispanic Multi-racial (two or more races).

2.2. Statistical Analysis

2.2.1. HVI Construction

Principal component analysis (PCA) was performed to reduce the original number of variables to a smaller number of sufficiently explanatory components. PCA reduces potential collinearity between original variables by grouping correlated variables into new principal components (Reid et al., 2009). The PCA method has been used previously to construct city-(Conlon et al., 2020; Johnson et al., 2012; Mallen et al., 2019; Wolf & McGregor, 2013), county-(Harlan et al., 2013; Prudent et al., 2016), state- (Maier et al., 2014; Nayak et al., 2018), and national-(Reid et al., 2009) level HVIs. The varimax rotation method minimizes the number of variables loading on specific principal components, ensuring they are independent of each other and the original variables (Reid et al., 2009). Principal components are retained if they meet each of the following standard criteria: a clear break in the Scree plot, Eigenvalue greater than 1, and the cumulative proportion of variance explained by the retained components is greater than 70% (Cattell, 1966; Jolliffe & Cadima, 2016; Wold et al., 1987). Census

tracts receive normalized factor scores for each retained component, which are often rescaled for easier interpretation and to minimize the effect of outliers in subsequent calculations (Reid et al., 2009).

We calculated an HVI for 55,267 census tracks, with 18,735 census tracts excluded from the analysis due to missing data for one or more variables. Together, the EVI and air temperature data sets contributed 15,927 (90.7%) of the missing data points, possibly due to grid cell disruption caused by water body or cloud coverage. Correlation among the included variables was assessed using Spearman's rank correlation coefficient (Table S1 in Supporting Information S1). PCA with varimax rotation identified five components to be retained based on meeting the standard criterion, adequately representing the various aspects of heat vulnerability (Figures S1 and S2 in Supporting Information S1). Factor loadings quantify each variable's influence on the individual retained components, and can be described as Education/Language, Economic/Demographic, Land Cover/Housing, Elderly/Social Isolation, and Exposure/Underlying Conditions factors (Table S2 in Supporting Information S1). For interpretability and calculation purposes, normalized factor scores produced from the varimax rotation were rescaled from 1 to 6 based on deviation from the mean. Each census tract, therefore, received five factor scores, each ranging from 1 to 6. The individual factor scores were summed to calculate the HVI score for each census tract, having a potential range of 5–30. Heat Vulnerability Index scores were geocoded and plotted using each census tract's unique GEOID.

2.2.2. Heat Vulnerability and Environmental Racism Analysis

Correlation and linear regression analysis methods were used to quantify the relationship between HVI scores and weighted HOLC scores at the census tract level. Weighted HOLC scores were rounded to the nearest integer and reassigned original grade measurements (1 = A, 2 = B, 3 = C, and 4 = D) to assess differences in HVI score among grade-specific strata. We used analysis of variance to test whether at least one HOLC grade-specific mean HVI score was significantly different from at least one other grade-specific score. If this was the case, we then used post-hoc honestly significant difference tests to calculate the magnitude, direction, and statistical significance of differences between HOLC grade-specific mean HVI scores. We compared mean HVI scores for CEJST "disadvantaged" and "non-disadvantaged" census tracts using the *t*-test. We used analysis of variance and post-hoc honestly significant difference tests to assess differences in mean HVI score among HOLC-grade specific census tract strata by CEJST disadvantaged community status.

Heat vulnerability was analyzed for the various race/ethnicity groups in the United States in several ways. First, a mean HVI score was calculated for each group weighted by the census-tract-specific population of each group. In addition, each census tract was assigned to a race/ethnicity category according to its modal, or most populous, race or ethnicity. Mean census tract HVI scores were then compared across race/ethnicity categories. For example, a census tract where 2,000 residents were Hispanic or Latino of any race, 1,000 were non-Hispanic White, 500 were non-Hispanic African American or Black, and 500 were non-Hispanic Asian, would be assigned to the Hispanic or Latino of any race category. The mean HVI score of all census tracts assigned to the Hispanic or Latino of any race category would be calculated and compared to that of other race/ethnicity categories. Finally, the population proportion of each race/ethnicity group was calculated for HVI score deciles.

3. Results

HVI scores were calculated for 55,267 U.S. census tracts (Figure 1). Scores ranged from 10 to 26 with a country-wide mean (SD) equal to 17.47 (2.16). Visual assessment of the HVI Map revealed higher HVI scores in urban census tracts compared to surrounding suburban and rural areas. In the greater New York City metropolitan area, higher HVI scores were apparent in the Bronx, Brooklyn, and Newark, New Jersey compared to lower scores in the western portion of Nassau County, New York, and Bergen County in northeastern New Jersey. In Chicago, high HVI scores were evident throughout Cook County, with lower scores more prevalent in the surrounding DuPage and Will Counties. Los Angeles and Houston's urban areas also exhibited considerably higher HVI scores than the surrounding suburbs. Figure 1 also depicts higher HVI scores in the southwestern United States, a spatial pattern consistent with the Global Burden of Disease (GBD) estimates of heat-related mortality at the state level (Figure S3 in Supporting Information S1) (Global Burden of Disease Study 2019 (GBD, 2019) Results, 2020). A sensitivity analysis was conducted to compare the original HVI scores, which used the average summertime 2m air temperature anomaly relative to the full-year MFT as the temperature anomaly variable, to alternative HVI scores using the average summertime 2m air temperature anomaly relative to the summertime
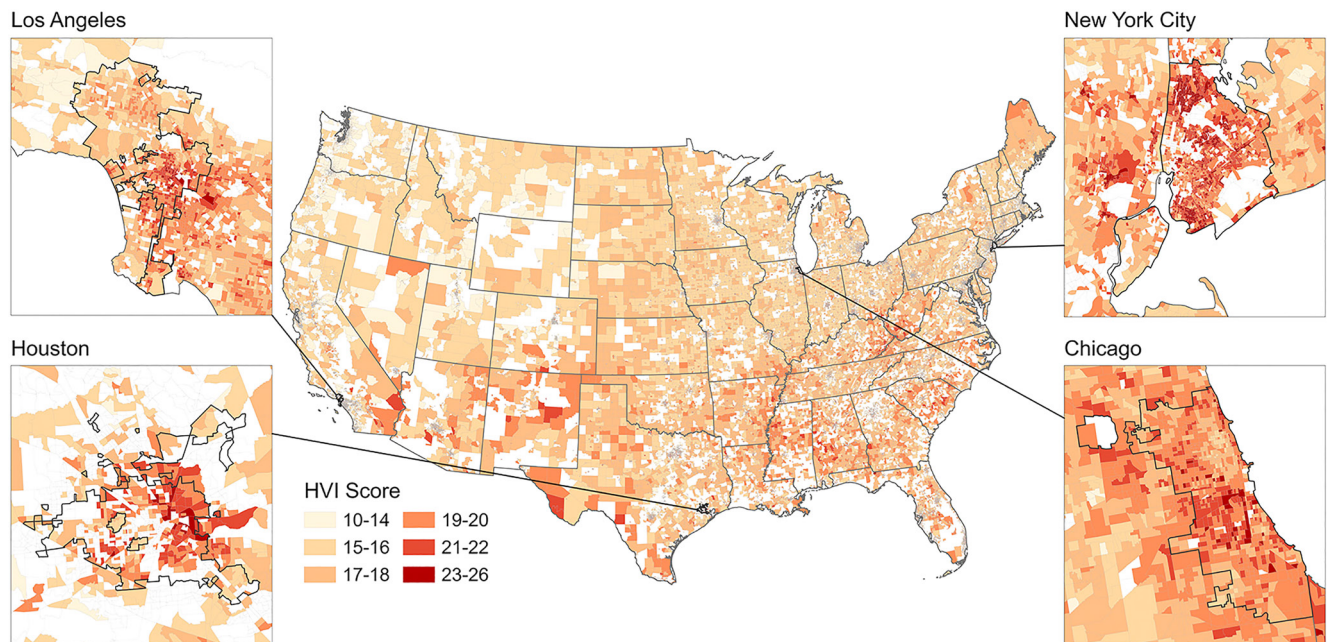
Figure 1. Heat Vulnerability Index (HVI) Score Maps. $N = 55,267$ census tracts. Census tracts with missing data for one or more variables were excluded from the analysis and did not receive an HVI score ($N = 18,735$; white color on the map). Enhanced vegetation index and air temperature were the primary contributors to missing data.

(June–August) MFT as the temperature anomaly variable. The sensitivity analysis yielded similar HVI results, with the original and alternative HVI scores highly correlated ($R = 0.88$) (Table S3 and Figure S4 in Supporting Information S1).

U.S. Department of Agriculture's Rural-Urban Commuting Area codes were used to assess differences in mean HVI scores between urban and non-urban areas (2010 Rural-Urban Commuting Area Codes, 2019). T test analysis measured significantly different (p-value < 0.001) mean HVI score in urban areas compared to non-urban areas. On average, HVI scores in urban areas were 0.29 (0.25, 0.33) points higher than in non-urban areas, supporting the visual differences apparent in Figure 1.

There was a weak-to-moderate association between HOLC grade and HVI (correlation coefficient of 0.305). Based on a simple linear model, per unit increase in weighted HOLC score was associated with a 0.8-point increase in HVI score (Figure S5 in Supporting Information S1). Mean (SD) HVI scores were 17.56 (1.80) for HOLC grade A census tracts, 18.61 (2.08) for grade B, 19.45 (1.92) for grade C, and 19.93 (1.90) for grade D (Figure 2). These mean HVI scores differed significantly across HOLC grade strata (p-value < 0.001). Post-hoc honestly significant difference tests calculated significantly higher (p-value < 0.001) HVI scores for each incrementally higher-risk HOLC grade, differing by 1.05 (0.81, 1.28) between "A" and "B," by 0.84 (0.71, 0.97) between "B" and "C," and by 0.48 (0.37, 0.60) between "C" and "D" (Figure 2).

We assessed the distribution of the raw HVI variables across the various HOLC grades using heat maps (Figure S6 in Supporting Information S1). Analysis of variance showed that the mean value of each raw HVI variable significantly differed across HOLC grades (Table S4 in Supporting Information S1), suggesting that each raw variable contributed to the difference in mean HVI scores across the HOLC grade strata.

The mean (SD) HVI score for CEJST-defined "disadvantaged" census tracts was 19.13 (1.89), significantly higher ($p < 0.001$) than the mean HVI score of 16.68 (1.80) for "non-disadvantaged" census tracts. We also calculated the mean HVI score for census tracts within each HOLC grade stratified by disadvantage community status and found the highest score for disadvantaged census tracts with HOLC grade "D" and the lowest for non-disadvantaged tracts with HOLC grade "A" (Figure 3). Analysis of variance showed that mean HVI scores significantly differed across HOLC grades among both the "disadvantaged" ($p < 0.001$) and "non-disadvantaged" ($p < 0.001$) census tracts. Incrementally higher-risk HOLC grades had significantly higher ($p < 0.001$) HVI score
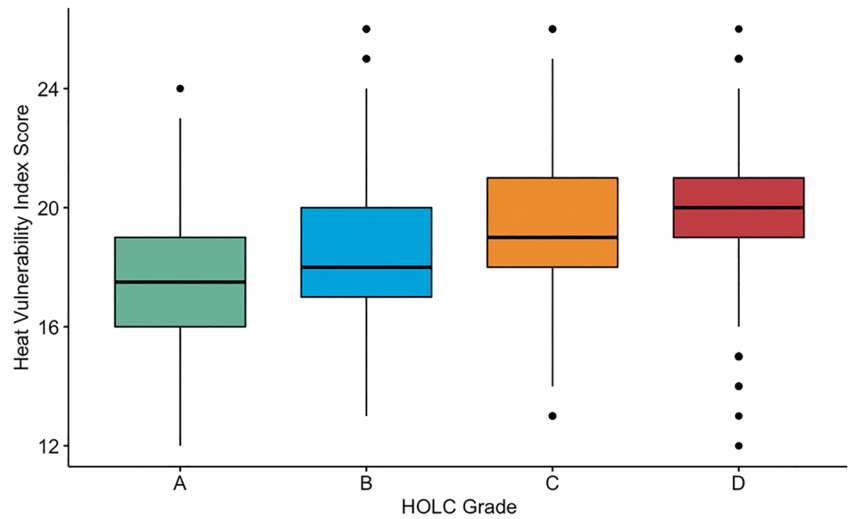
Figure 2. Distribution of Census Tract Heat Vulnerability Index (HVI) Scores for Home Owners Loan Corporation (HOLC) Grades. "HOLC Grade" x-axis label represents HOLC lending risk grade. Grade D represents historically "redlined" census tracts. Differences in HVI scores between adjacent HOLC grades were statistically significant (p-value < 0.001) according to post-hoc honest significant difference tests. Boxes depict HVI score interquartile range for each HOLC grade stratum. The middle line within the box marks the median HVI score for each HOLC grade. $N = 10{,}701$ census tracts with both a HOLC grade and complete data to calculate an HVI score.

among non-disadvantaged census tracts. However, the only significant difference among disadvantaged tracts was between grade "C" and grade "D." Within each HOLC grade stratum, disadvantaged census tracts had a significantly higher ($p < 0.001$) mean HVI score than non-disadvantaged tracts.
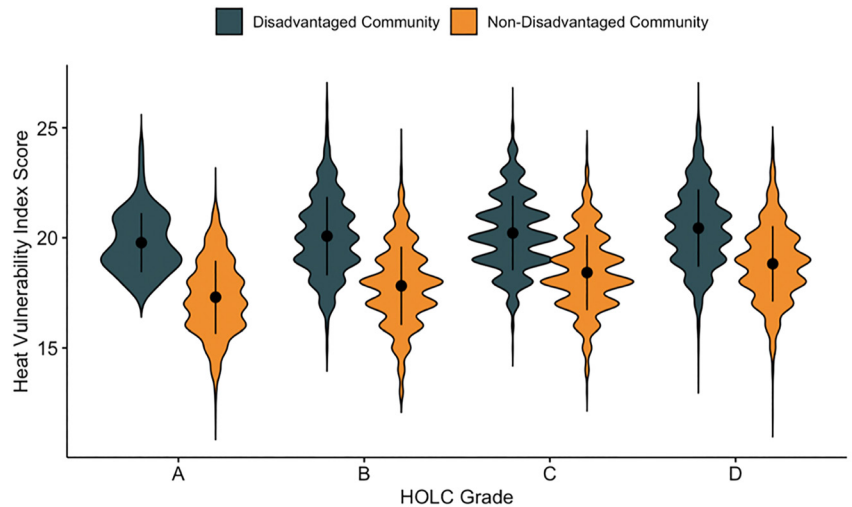
Mean (SD) Heat Vulnerability Index Scores

	A	B	C	D	ANOVA p-value
Disadvantaged Community	19.8 (1.3)	20.1 (1.8)	20.2 (1.7)	20.4 (1.8)	< 0.001
Non-Disadvantaged Community	17.3 (1.7)	17.8 (1.8)	18.4 (1.7)	18.8 (1.7)	< 0.001

Figure 3. Heat Vulnerability Index (HVI) Scores for Disadvantaged Communities and Home Owners Loan Corporation (HOLC) Grades. Violin plots show the density of census tracts receiving a particular HVI score given their HOLC grade and disadvantaged community status. Wider portions of the violin indicate more census tracts with the corresponding HVI score, while narrower portions indicate fewer census tracts with corresponding HVI score. The black dot and error bar within each violin mark the mean HVI score and standard deviation for each HOLC grade and disadvantaged community status stratum. $N = 10{,}701$ census tracts with both a HOLC grade and complete data to calculate an HVI score.
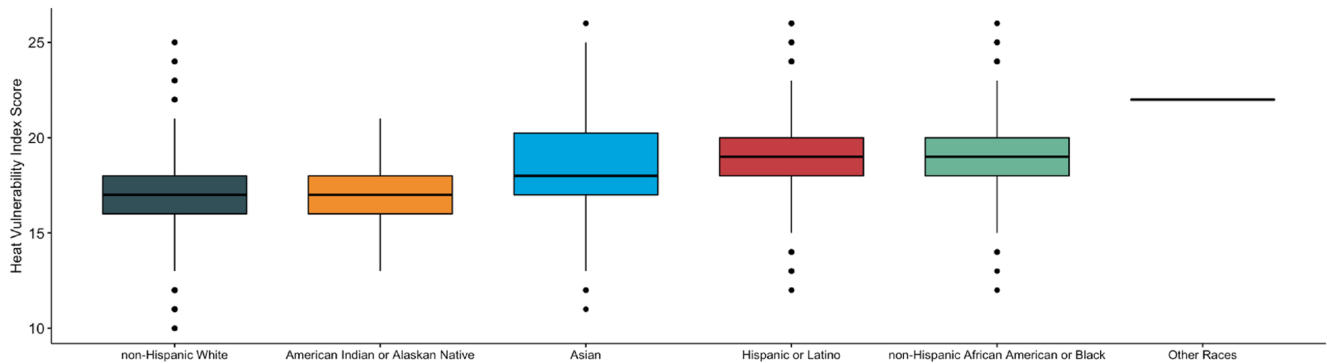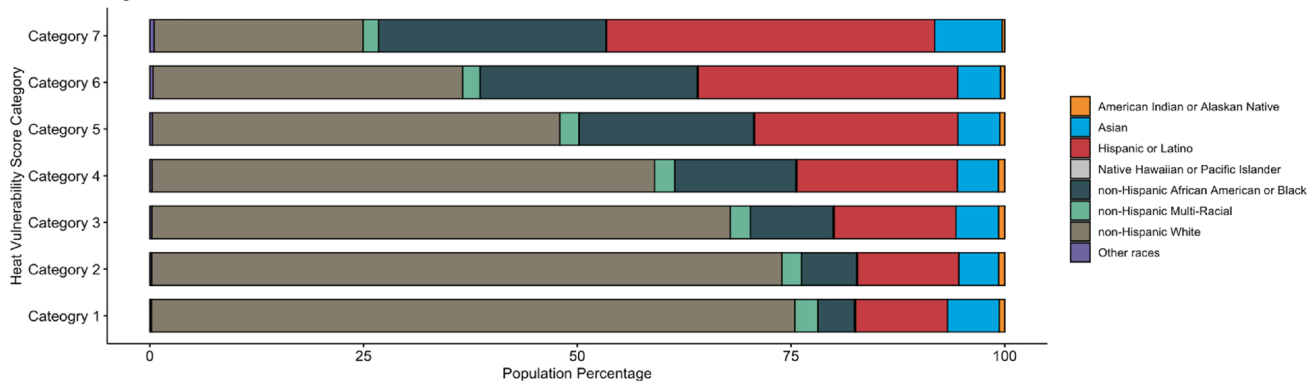
Figure 4. Heat Vulnerability Index (HVI) Scores for Race/Ethnicity Groups. (a) Boxes depict HVI score interquartile range for each race/ethnicity group. The middle line within the box marks the median HVI score. The Native Hawaiian or Pacific Islander and Multi-race groups were not included because neither was the modal group in any census tract. (b) Bar plot depicts the race/ethnicity group population proportions within each HVI score category. Category "1" represents the lowest HVI scores and category "7" represents the highest HVI scores. These are the HVI score ranges corresponding to each category: category 1: 10–15 (N = 9,497; 18.6%); category 2: 16 (N = 8,313; 16.3%); category 3: 17 (N = 9,380; 18.4%); category 4: 18 (N = 8,935; 17.5%); category 5: 19 (N = 6,600; 12.9%); category 6: 20 (N = 4,180; 8.2%); and category 7: 21–26 (N = 4,124; 8.1%). N = census tracts.

The mean (SD) HVI score was highest for the non-Hispanic Black or African American race/ethnicity group at 18.51 (2.02), followed by 18.19 (2.29) for Hispanic or Latino of any race, 17.95 (2.29) for Other races, 17.31 (2.44) for Asian, 17.05 (1.90) for American Indian or Alaskan Native, 17.05 (2.14) for Multi-race, and 16.76 (1.90) for non-Hispanic White, and 16.76 (2.13) for Native Hawaiian or Pacific Islander. These mean HVI scores differed significantly ($p = 0.036$) across groups. When calculated based on the modal race/ethnicity group population in each census tract, the mean (SD) HVI score was highest for Other races at 22.0 (0.0) (based on only two census tracts in which Other races had the modal population), followed by 19.31 (1.70) for non-Hispanic Black or African American, 19.06 (2.14) for Hispanic or Latino of any race, 18.51 (2.66) for Asian, 16.96 (1.71) for American Indian or Alaskan Native, and 16.90 (1.89) for non-Hispanic White (Figure 4a). The Native Hawaiian or Pacific Islander and Multi-race race/ethnicity groups were not the modal population in any census tract.

Non-white persons were overrepresented in the most heat-vulnerable census tracts (Figure 4b). Non-white individuals made up 75.6% of the population in the highest HVI score category of census tracts, compared to only 24.7% in the lowest category. Hispanic or Latino and non-Hispanic African American or Black individuals accounted for 38.4% and 26.6% of the highest category population, respectively, compared to 10.7% and 4.3% in the lowest category population and 18.0% and 12.3% in the entire United States population (ACS Demographic and Housing Estimates, 2019).

4. Discussion

The analyses in this study each supported the hypothesis that vulnerability to heat-related adverse health outcomes is greatest in historically defined and contemporaneously defined disadvantaged communities and in communities of color in the United States. Historically "redlined" census tracts were associated with higher heat vulnerability,

consistent with similar analyses that found higher LST and lower green space in these segregated areas (Hoffman et al., 2020; Li et al., 2021; Namin et al., 2020; Nardone et al., 2021; Schinasi et al., 2022; Wilson, 2020). This association was evidenced by the correlation and regression analyses between continuous, weighted HOLC score and HVI score, as well as significantly increasing HVI scores between incrementally higher-risk HOLC grades. These residential disparities were driven by inequitably distributed determinants of heat vulnerability (i.e., the raw HVI variables), each of which differed significantly among HOLC grade strata.

Contemporaneously defined disadvantaged community status was also found to be associated with higher HVI score, both in aggregate and across HOLC grade strata. When HOLC grade and CEJST disadvantaged community status were assessed together, the highest place-based heat vulnerability was measured in census tracts that were both historically redlined and presently disadvantaged. Finally, we observed high mean HVI scores among non-White race/ethnicity groups, and overrepresentation of people of color in the most vulnerable census tracts. Together, these results demonstrate place- and race/ethnicity-based disparities in heat vulnerability across the United States, and add to the literature on the long-term adverse environmental and health implications associated with racist housing policies (Hoffman et al., 2020; Li et al., 2021; Namin et al., 2020; Nardone et al., 2021; Schinasi et al., 2022; Wilson, 2020).

In addition to residential and race/ethnicity differences in heat vulnerability, urban areas were measured to have higher HVI scores than non-urban areas. This difference in vulnerability, however, cannot be validated without nationwide estimates of heat-related mortality. Although previous heat vulnerability indices also have measured increased vulnerability in urban areas (Reid et al., 2009), other studies have identified higher risk of heat mortality in rural areas (Chen et al., 2016; Hu et al., 2019). Heat vulnerability in urban versus non-urban communities has complex differences; therefore adaptation strategies should be designed to target the specific needs of each area.

The HVI developed in this study utilizes methodologies applied in previous studies (Reid et al., 2009), but also builds on previous indices in several ways. First, constructing the index with data from the most recently updated data sets provides more temporally relevant measures of the included variables. Utilizing the most recent temperature estimates in particular is crucial for adequately describing heat exposure, as warming trends differ between the most and least socially vulnerable counties in the United States (Spangler & Wellenius, 2020). Second, the air temperature variable used to construct our HVI measures heat exposure more accurately (World Health Organization, 2021) than does LST, which has been used in the construction of previous indices. LST likely misrepresents heat exposure, as atmospheric and surface conditions can cause several degree differences between LST and ambient air temperature (Good, 2016). Additionally, measuring heat exposure based on recent summer months' temperature anomaly relative to the MFT captures current and spatially diverse warming trends. Basing the temperature anomaly on MFT, which is closely associated with minimum mortality temperature, also helps take into account potential geography-specific temperature adaptation, making it a multifaceted measure of heat exposure (Yin et al., 2019). Finally, this assessment provides HVI scores for most United States' census tracts ($n = 55,267$; 75% of census tracts), capturing vulnerability across urban, suburban, and rural areas. An earlier study sought to measure heat vulnerability for the entire country but excluded many non-urban areas from the final vulnerability scores due to the lack of a nationwide data set for air conditioning (Reid et al., 2009). Other studies of heat vulnerability within individual cities (Conlon et al., 2020; Johnson et al., 2012; Mallen et al., 2019; Wolf & McGregor, 2013), counties (Harlan et al., 2013; Prudent et al., 2016), or states (Maier et al., 2014; Nayak et al., 2018) did not provide the national scope necessary for an environmental racism assessment.

Beyond the improvements to the HVI, this study provided a unique analysis of the place- and race/ethnicity-based disparities associated with heat vulnerability. Previous studies have measured higher LST and lower green space in "redlined" areas (Hoffman et al., 2020; Li et al., 2021; Namin et al., 2020; Nardone et al., 2021; Schinasi et al., 2022; Wilson, 2020), but these studies failed to capture the various other socioeconomic, demographic, or biological determinants of vulnerability (World Health Organization, 2021). Additionally, this study is the first to quantify heat vulnerability across the various race/ethnicity groups in the United States, further illustrating the vulnerability of communities of color.

This study had several limitations. First, 18,735 census tracts did not receive an HVI score due to missing data and were therefore excluded from the analysis. Data loss occurred primarily during the calculation of census tract level EVI and air temperature values, possibly due to grid cell disruption caused by cloud coverage (Shen et al., 2015). We cannot rule out the possibility of some selection bias due to exclusion of these census tracts.

A second limitation was the lack of a nationwide data set measuring census-tract-level air conditioning access, which is known to provide strong protection against heat-related morbidity and mortality (Bouchama et al., 2007; Kaiser et al., 2001; Kilbourne et al., 1982; Naughton et al., 2002; Petkova et al., 2014; Romanello et al., 2021; Semenza et al., 1996). The positive association that has been observed between warmer temperatures and air conditioning access could indicate more widespread access to air conditioning across the southern portion of the country, further influencing the spatial distribution of HVI scores across the United States if air conditioning access had been included as a variable in the HVI construction (Bell et al., 2009). A third limitation was the use of diabetes to represent all comorbidities and underlying health conditions associated with heat-related morbidity and mortality. In fact, the magnitude of the association between heat exposure and various physical and mental health conditions varies (Knowlton et al., 2009; Semenza et al., 1996, 1999); however, measures of underlying health conditions other than diabetes were unavailable nationally at the county- or census-tract-level. Additionally, the original variables used to construct the HVI were consistent across geographic locations, but heat vulnerability in urban versus non-urban areas could be dependent on which combination of raw variables are used (Fard et al., 2021). Though a potential limitation, the observed urban versus non-urban differences in heat vulnerability are likely driven by differences in exposure, susceptibility, and adaptability that are captured in the original variables.

A fourth limitation of this study was that we were unable to validate the HVI by comparison to actual empirical heat-related morbidity or mortality data, due to data unavailability, but the general spatial pattern of HVI scores had approximate consistency with the GBD estimates of heat-related mortality at the state level (Global Burden of Disease Study 2019 (GBD, 2019) Results, 2020). A further limitation was that the Home Owners' Loan Corporation assigned grades based on the demographic, economic and social construction of a neighborhood, implicitly taking into account many of the same variables used for construction of the HVI score (Nardone et al., 2021; Pearcy, 2020). Finally, the White House Council on Environmental Quality's CEJST, which was utilized for this analysis due to its national scope, did not include race/ethnicity as a criterion for identifying environmentally and socially disadvantaged communities in the United States. Race/ethnicity also is not taken into account in California's CalEnviroScreen (CalEnviroScreen 4.0, 2021), but is a factor in the New York State Disadvantage Communities Map (Disadvantaged Communities Map, 2022). Due to varying geographic domains, a unique combination of demographic, socioeconomic, and environmental determinants, as well as different development methodologies, comparing our HVI scores to disadvantaged community status defined by these other tools would result in different outcomes and conclusions.

5. Conclusion

Residential and racial inequalities associated with heat vulnerability identified by this study confirm the persistent legacy of racist policies in the United States and their connection to contemporary environmental injustices. Our findings can help inform policymakers about the national distribution of place- and race-based disparities in heat vulnerability to develop equity-promoting climate adaptation policies.

Conflict of Interest

The authors declare no conflicts of interest relevant to this study.

Data Availability Statement

Data on the heat vulnerability index and its indicators are publicly available at Zenodo (https://doi.org/10.5281/zenodo.7141231).

References

2010 Rural-Urban Commuting Area Codes. (2019). [CSV Data File]. Retrieved from https://www.ers.usda.gov/data-products/rural-urban-commuting-area-codes/

Aaronson, D., Hartley, D., & Mazumder, B. (2021). The effects of the 1930s HOLC "redlining" maps. *American Economic Journal: Economic Policy*, *13*(4), 355–392. https://doi.org/10.1257/pol.20190414

ACS Demographic and Housing Estimates. (2019). [CSV Data File]. U.S. Census Bureau. Retrieved from https://data.census.gov/cedsci/table?q=demographic%26g=0100000US%241400000%26tid=ACSDP5Y2019.DP05

Age and Sex. (2019). [CSV Data File]. U.S. Census Bureau. Retrieved from https://data.census.gov/cedsci/table?q=age%20and%20sex%26g=01 00000US%241400000%26tid=ACSST5Y2019.S0101

Anderson, B. G., & Bell, M. L. (2009). Weather-related mortality: How heat, cold, and heat waves affect mortality in the United States. *Epidemiology*, *20*(2), 205–213. https://doi.org/10.1097/EDE.0b013e318190ee08

Avashia, V., Garg, A., & Dholakia, H. (2021). Understanding temperature related health risk in context of urban land use changes. *Landscape and Urban Planning*, *212*, 104107. https://doi.org/10.1016/j.landurbplan.2021.104107

Bark, N. (1998). Deaths of psychiatric patients during heat waves. *Psychiatric Services*, *49*(8), 1088–1090. https://doi.org/10.1176/ps.49.8.1088

Bark, N. M. (1982). The prevention and treatment of heatstroke in psychiatric patients. *Hospital and Community Psychiatry*, *33*(6), 474–476. https://doi.org/10.1176/ps.33.6.474

Basu, R., Feng, W. Y., & Ostro, B. D. (2008). Characterizing temperature and mortality in nine California counties. *Epidemiology*, *19*(1), 138–145. https://doi.org/10.1097/EDE.0b013e31815c1da7

Bell, M. L., Ebisu, K., Peng, R. D., & Dominici, F. (2009). Adverse health effects of particulate air pollution: Modification by air conditioning. *Epidemiology*, *20*(5), 682–686. https://doi.org/10.1097/EDE.0b013e3181aba749

Bouchama, A., Dehbi, M., Mohamed, G., Matthies, F., Shoukri, M., & Menne, B. (2007). Prognostic factors in heat wave–related deaths: A meta-analysis. *Archives of Internal Medicine*, *167*(20), 2170–2176. https://doi.org/10.1001/archinte.167.20.ira70009

Bravo, M. A., Anthopolos, R., Bell, M. L., & Miranda, M. L. (2016). Racial isolation and exposure to airborne particulate matter and ozone in understudied US populations: Environmental justice applications of downscaled numerical model output. *Environment International*, *92–93*, 247–255. https://doi.org/10.1016/j.envint.2016.04.008

Buechley, R. W., Van Bruggen, J., & Truppi, L. E. (1972). Heat island equals death island? *Environmental Research*, *5*(1), 85–92. https://doi.org/10.1016/0013-9351(72)90022-9

CalEnviroScreen 4.0. (2021). Office of Environmental Health Hazard Assessment. Retrieved from https://oehha.ca.gov/calenviroscreen/report/calenviroscreen-40

Campbell, S., Remenyi, T. A., White, C. J., & Johnston, F. H. (2018). Heatwave and health impact research: A global review. *Health & Place*, *53*, 210–218. https://doi.org/10.1016/j.healthplace.2018.08.017

Cattell, R. B. (1966). The scree test for the number of factors. *Multivariate Behavioral Research*, *1*(2), 245–276. https://doi.org/10.1207/s15327906mbr0102_10

Chavis, B. F. (1994). Preface. In R. D. Bullard (Ed.), *Unequal protection: Environmental justice and communities of color*, (pp. xi–xii). Sierra Club Books.

Chen, K., Zhou, L., Chen, X., Ma, Z., Liu, Y., Huang, L., et al. (2016). Urbanization level and vulnerability to heat-related mortality in Jiangsu Province, China. *Environmental Health Perspectives*, *124*(12), 1863–1869. https://doi.org/10.1289/EHP204

Chow, W. T. L., Chuang, W.-C., & Gober, P. (2012). Vulnerability to extreme heat in metropolitan Phoenix: Spatial, temporal, and demographic dimensions. *The Professional Geographer*, *64*(2), 286–302. https://doi.org/10.1080/00330124.2011.600225

Clarke, J. F. (1972). Some effects of the urban structure on heat mortality. *Environmental Research*, *5*(1), 93–104. https://doi.org/10.1016/0013-9351(72)90023-0

Clarke, P., & Melendez, R. (2019). *National neighborhood data archive (NaNDA): Land Cover by census tract, United States, 2001–2016* (version 1). Inter-University Consortium for Political and Social Research. https://doi.org/10.3886/E110663V1

Climate and Economic Justice Screening Tool. (2022a). Council on Environmental Quality. Retrieved from https://screeningtool.geoplatform.gov/en/methodology

Climate and Economic Justice Screening Tool. (2022b). [CSV Data File]. Retrieved from https://screeningtool.geoplatform.gov/en/downloads

Conlon, K. C., Mallen, E., Gronlund, C. J., Berrocal, V. J., Larsen, L., & O'Neill, M. S. (2020). Mapping human vulnerability to extreme heat: A critical assessment of heat vulnerability indices created using principal components analysis. *Environmental Health Perspectives*, *128*(9), 097001. https://doi.org/10.1289/EHP4030

Curriero, F. C., Heiner, K. S., Samet, J. M., Zeger, S. L., Strug, L., & Patz, J. A. (2002). Temperature and mortality in 11 cities of the eastern United States. *American Journal of Epidemiology*, *155*(1), 80–87. https://doi.org/10.1093/aje/155.1.80

Didan, K. (2015). MOD13A2 MODIS/Terra vegetation indices 16-day L3 global 1km SIN grid V006 [Dataset]. NASA EOSDIS Land Processes DAAC. https://doi.org/10.5067/MODIS/MOD13A2.006

Disadvantaged Communities Map. (2022). New York State Department of Environmental Conservation. Retrieved from https://climate.ny.gov/Our-Climate-Act/Disadvantaged-Communities-Criteria/Disadvantaged-Communities-Map

Fard, B. J., Mahmood, R., Hayes, M., Rowe, C., Abadi, A. M., Shulski, M., et al. (2021). Mapping heat vulnerability index based on different urbanization levels in Nebraska, USA. *GeoHealth*, *5*(10), e2021GH000478. https://doi.org/10.1029/2021GH000478

Gee, G. C., & Payne-Sturges, D. C. (2004). Environmental health disparities: A framework integrating psychosocial and environmental concepts. *Environmental Health Perspectives*, *112*(17), 1645–1653. https://doi.org/10.1289/ehp.7074

Global Burden of Disease Study 2019 (GBD 2019) Results. (2020). Institute for Health Metrics and Evaluation (IHME). Retrieved from https://vizhub.healthdata.org/gbd-results/

Good, E. J. (2016). An in situ-based analysis of the relationship between land surface "skin" and screen-level air temperatures. *Journal of Geophysical Research: Atmospheres*, *121*(15), 8801–8819. https://doi.org/10.1002/2016JD025318

Gronlund, C. J., Berrocal, V. J., White-Newsome, J. L., Conlon, K. C., & O'Neill, M. S. (2015). Vulnerability to extreme heat by socio-demographic characteristics and area green space among the elderly in Michigan, 1990–2007. *Environmental Research*, *136*, 449–461. https://doi.org/10.1016/j.envres.2014.08.042

Gronlund, C. J., Zanobetti, A., Wellenius, G. A., Schwartz, J. D., & O'Neill, M. S. (2016). Vulnerability to renal, heat and respiratory hospitalizations during extreme heat among U.S. elderly. *Climate Change*, *136*(3), 631–645. https://doi.org/10.1007/s10584-016-1638-9

Hansen, A., Bi, L., Saniotis, A., & Nitschke, M. (2013). Vulnerability to extreme heat and climate change: Is ethnicity a factor? *Global Health Action*, *6*(1), 21364. https://doi.org/10.3402/gha.v6i0.21364

Harlan, S. L., Brazel, A. J., Prashad, L., Stefanov, W. L., & Larsen, L. (2006). Neighborhood microclimates and vulnerability to heat stress. *Social Science & Medicine*, *63*(11), 2847–2863. https://doi.org/10.1016/j.socscimed.2006.07.030

Harlan, S. L., Declet-Barreto, J. H., Stefanov, W. L., & Petitti, D. B. (2013). Neighborhood effects on heat deaths: Social and environmental predictors of vulnerability in Maricopa County, Arizona. *Environmental Health Perspectives*, *121*(2), 197–204. https://doi.org/10.1289/ehp.1104625

Hoffman, J. S., Shandas, V., & Pendleton, N. (2020). The effects of historical housing policies on resident exposure to intra-urban heat: A study of 108 US urban areas. *Climate*, *8*(1), 12. https://doi.org/10.3390/cli8010012

Hu, K., Guo, Y., Hochrainer-Stigler, S., Liu, W., See, L., Yang, X., et al. (2019). Evidence for urban-rural disparity in temperature-mortality relationships in Zhejiang Province, China. *Environmental Health Perspectives*, *127*(3), 037001. https://doi.org/10.1289/EHP3556

Iglay, K., Hannachi, H., Joseph Howie, P., Xu, J., Li, X., Engel, S. S., et al. (2016). Prevalence and co-prevalence of comorbidities among patients with type 2 diabetes mellitus. *Current Medical Research and Opinion*, *32*(7), 1243–1252. https://doi.org/10.1185/03007995.2016.1168291

Johnson, D. P., & Wilson, J. S. (2009). The socio-spatial dynamics of extreme urban heat events: The case of heat-related deaths in Philadelphia. *Applied Geography*, *29*(3), 419–434. https://doi.org/10.1016/j.apgeog.2008.11.004

Johnson, D. P., Stanforth, A., Lulla, V., & Luber, G. (2012). Developing an applied extreme heat vulnerability index utilizing socioeconomic and environmental data. *Applied Geography*, *35*(1), 23–31. https://doi.org/10.1016/j.apgeog.2012.04.006

Jolliffe, I. T., & Cadima, J. (2016). Principal component analysis: A review and recent developments. *Philosophical Transactions of the Royal Society A: Mathematical, Physical and Engineering Sciences*, *374*(2065), 1–16. https://doi.org/10.1098/rsta.2015.0202

Jones, T. S., Liang, A. P., Kilbourne, E. M., Griffin, M. R., Patriarca, P. A., Wassilak, S. G., et al. (1982). Morbidity and mortality associated with the July 1980 heat wave in St Louis and Kansas City, Mo. *Jama*, *247*(24), 3327–3331. https://doi.org/10.1001/jama.247.24.3327

Kaiser, R., Rubin, C. H., Henderson, A. K., Wolfe, M. I., Kieszak, S., Parrott, C. L., & Adcock, M. (2001). Heat-related death and mental illness during the 1999 Cincinnati heat wave. *The American Journal of Forensic Medicine and Pathology*, *22*(3), 303–307. https://doi.org/10.1097/00000433-200109000-00022

Kilbourne, E. M., Choi, K., Jones, T. S., & Thacker, S. B. (1982). Risk factors for heatstroke: A case-control study. *Jama*, *247*(24), 3332–3336. https://doi.org/10.1001/jama.1982.03320490030031

Knowlton, K., Rotkin-Ellman, M., King, G., Margolis, H. G., Smith, D., Solomon, G., et al. (2009). The 2006 California heat wave: Impacts on hospitalizations and emergency department visits. *Environmental Health Perspectives*, *117*(1), 61–67. https://doi.org/10.1289/ehp.11594

Li, D., Newman, G. D., Wilson, B., Zhang, Y., & Brown, R. D. (2021). Modeling the relationships between historical redlining, urban heat, and heat-related emergency department visits: An examination of 11 Texas cities. *Environment and Planning B: Urban Analytics and City Science*, *49*(3), 933–952. https://doi.org/10.1177/23998083211039854

Lin, S., Luo, M., Walker, R. J., Liu, X., Hwang, S. A., & Chinery, R. (2009). Extreme high temperatures and hospital admissions for respiratory and cardiovascular diseases. *Epidemiology*, *20*(5), 738–746. https://doi.org/10.1097/EDE.0b013e3181ad5522

Lopez, R. (2002). Segregation and black/white differences in exposure to air toxics in 1990. *Environmental Health Perspectives*, *110*(Suppl 2), 289–295. https://doi.org/10.1289/ehp.02110s2289

Maier, G., Grundstein, A., Jang, W., Li, C., Naeher, L. P., & Shepherd, M. (2014). Assessing the performance of a vulnerability index during oppressive heat across Georgia, United States. *Weather, Climate, and Society*, *6*(2), 253–263. https://doi.org/10.1175/wcas-d-13-00037.1

Mallen, E., Stone, B., & Lanza, K. (2019). A methodological assessment of extreme heat mortality modeling and heat vulnerability mapping in Dallas, Texas. *Urban Climate*, *30*, 100528. https://doi.org/10.1016/j.uclim.2019.100528

McGeehin, M. A., & Mirabelli, M. (2001). The potential impacts of climate variability and change on temperature-related morbidity and mortality in the United States. *Environmental Health Perspectives*, *109*(Suppl 2), 185–189. https://doi.org/10.1289/ehp.109-1240665

Medina-Ramón, M., & Schwartz, J. (2007). Temperature, temperature extremes, and mortality: A study of acclimatisation and effect modification in 50 US cities. *Occupational and Environmental Medicine*, *64*(12), 827–833. https://doi.org/10.1136/oem.2007.033175

Meier, H. C. S., & Mitchell, B. C. (2021). *Historic redlining scores for 2010 and 2020 US census tracts* (version 1). Inter-University Consortium for Political and Social Research. https://doi.org/10.3886/E141121V1

Morello-Frosch, R., & Jesdale, B. M. (2006). Separate and unequal: Residential segregation and estimated cancer risks associated with ambient air toxics in U.S. metropolitan areas. *Environmental Health Perspectives*, *114*(3), 386–393. https://doi.org/10.1289/ehp.8500

Namin, S., Xu, W., Zhou, Y., & Beyer, K. (2020). The legacy of the Home Owners' Loan Corporation and the political ecology of urban trees and air pollution in the United States. *Social Science & Medicine*, *246*, 112758. https://doi.org/10.1016/j.socscimed.2019.112758

Nardone, A., Rudolph, K. E., Morello-Frosch, R., & Casey, J. A. (2021). Redlines and greenspace: The relationship between historical redlining and 2010 greenspace across the United States. *Environmental Health Perspectives*, *129*(1), 17006. https://doi.org/10.1289/EHP7495

Naughton, M. P., Henderson, A., Mirabelli, M. C., Kaiser, R., Wilhelm, J. L., Kieszak, S. M., et al. (2002). Heat-related mortality during a 1999 heat wave in Chicago. *American Journal of Preventive Medicine*, *22*(4), 221–227. https://doi.org/10.1016/s0749-3797(02)00421-x

Nawrot, T. S., Torfs, R., Fierens, F., De Henauw, S., Hoet, P. H., Van Kersschaever, G., et al. (2007). Stronger associations between daily mortality and fine particulate air pollution in summer than in winter: Evidence from a heavily polluted region in western Europe. *Journal of Epidemiology & Community Health*, *61*(2), 146–149. https://doi.org/10.1136/jech.2005.044263

Nayak, S. G., Shrestha, S., Kinney, P. L., Ross, Z., Sheridan, S. C., Pantea, C. I., et al. (2018). Development of a heat vulnerability index for New York State. *Public Health*, *161*, 127–137. https://doi.org/10.1016/j.puhe.2017.09.006

Nelson, R. K., Winling, L., Marciano, R., Connolly, N., & Ayers, E. L. (2020). *Mapping inequality: Redlining in new deal America*. American Panorama. Retrieved from http://dsl.richmond.edu/panorama/redlining/#text=downloads

O'Neill, M. S., Zanobetti, A., & Schwartz, J. (2003). Modifiers of the temperature and mortality association in seven US cities. *American Journal of Epidemiology*, *157*(12), 1074–1082. https://doi.org/10.1093/aje/kwg096

O'Neill, M. S., Zanobetti, A., & Schwartz, J. (2005). Disparities by race in heat-related mortality in four US cities: The role of air conditioning prevalence. *Journal of Urban Health*, *82*(2), 191–197. https://doi.org/10.1093/jurban/jti043

Pearcy, M. (2020). "The most insidious legacy"—Teaching about redlining and the impact of racial residential segregation. *The Geography Teacher*, *17*(2), 44–55. https://doi.org/10.1080/19338341.2020.1759118

Perry, R. J. (2007). *"Race" and racism: The development of modern racism in America*. Palgrave Macmillan.

Petkova, E. P., Gasparrini, A., & Kinney, P. L. (2014). Heat and mortality in New York City since the beginning of the 20th century. *Epidemiology*, *25*(4), 554–560. https://doi.org/10.1097/EDE.0000000000000123

Physical Housing Characteristics for Occupied Housing Units. (2019). [CVS Data File]. U.S. Census Bureau. Retrieved from https://data.census.gov/cedsci/table?q=housing%26g=0100000US%241400000%26tid=ACSST5Y2019.S2504

Poverty Status in the Past 12 Months. (2019). [CVS Data File]. U.S. Census Bureau. Retrieved from https://data.census.gov/cedsci/table?q=poverty%26g=0100000US%241400000%26tid=ACSST5Y2019.S1701

Prudent, N., Houghton, A., & Luber, G. (2016). Assessing climate change and health vulnerability at the local level: Travis County, Texas. *Disasters*, *40*(4), 740–752. https://doi.org/10.1111/disa.12177

Qian, Z., He, Q., Lin, H.-M., Kong, L., Bentley, C. M., Liu, W., & Zhou, D. (2008). High temperatures enhanced acute mortality effects of ambient particle pollution in the "oven" city of Wuhan, China. *Environmental Health Perspectives*, *116*(9), 1172–1178. https://doi.org/10.1289/ehp.10847

Reid, C. E., O'Neill, M. S., Gronlund, C. J., Brines, S. J., Brown, D. G., Diez-Roux, A. V., & Schwartz, J. (2009). Mapping community determinants of heat vulnerability. *Environmental Health Perspectives*, *117*(11), 1730–1736. https://doi.org/10.1289/ehp.0900683

Romanello, M., McGushin, A., Claudia Di, N., Drummond, P., Hughes, N., Jamart, L., et al. (2021). The 2021 report of the Lancet Countdown on health and climate change: Code red for a healthy future. *Lancet*, *398*(10311), 1619–1662. https://doi.org/10.1016/S0140-6736(21)01787-6

Schinasi, L. H., Kanungo, C., Christman, Z., Barber, S., Tabb, L., & Headen, I. (2022). Associations between historical redlining and present-day heat vulnerability housing and land cover characteristics in Philadelphia, PA. *Journal of Urban Health*, *99*(1), 134–145. https://doi.org/10.1007/s11524-021-00602-6

Schwartz, J. (2005). Who is sensitive to extremes of temperature?: A case-only analysis. *Epidemiology*, *16*(1), 67–72. https://doi.org/10.1097/01.ede.0000147114.25957.71

Selected Economic Characteristics. (2019). [CSV Data File]. U.S. Census Bureau. Retrieved from https://data.census.gov/cedsci/table?q=economic%26g=0100000US%241400000%26tid=ACSDP5Y2019.DP03

Selected Social Characteristics in the United States. (2019). [CSV Data File]. U.S. Census Bureau. Retrieved from https://data.census.gov/table?q=aCSDP5Y2019.DP02

Semenza, J. C., McCullough, J. E., Flanders, W. D., McGeehin, M. A., & Lumpkin, J. R. (1999). Excess hospital admissions during the July 1995 heat wave in Chicago. *American Journal of Preventive Medicine*, *16*(4), 269–277. https://doi.org/10.1016/s0749-3797(99)00025-2

Semenza, J. C., Rubin, C. H., Falter, K. H., Selanikio, J. D., Flanders, W. D., Howe, H. L., & Wilhelm, J. L. (1996). Heat-related deaths during the July 1995 heat wave in Chicago. *New England Journal of Medicine*, *335*(2), 84–90. https://doi.org/10.1056/NEJM199607113350203

Shen, H., Li, X., Cheng, Q., Zeng, C., Yang, G., Li, H., & Zhang, L. (2015). Missing information reconstruction of remote sensing data: A technical review. *IEEE Transactions on Geoscience and Remote Sensing*, *3*(3), 61–85. https://doi.org/10.1109/MGRS.2015.2441912

Smoyer, K. E. (1998). Putting risk in its place: Methodological considerations for investigating extreme event health risk. *Social Science & Medicine*, *47*(11), 1809–1824. https://doi.org/10.1016/S0277-9536(98)00237-8

Spangler, K. R., & Wellenius, G. A. (2020). Spatial patterns of recent US summertime heat trends: Implications for heat sensitivity and health adaptations. *Environmental Research Communications*, *2*(3), 035002. https://doi.org/10.1088/2515-7620/ab7abb

Thornton, M. M., Shrestha, R., Wei, Y., Thornton, P. E., Kao, S., & Wilson, B. E. (2020). Daymet: Daily surface weather data on a 1-km grid for North America, version 4. https://doi.org/10.3334/ORNLDAAC/2129

Uejio, C. K., Wilhelmi, O. V., Golden, J. S., Mills, D. M., Gulino, S. P., & Samenow, J. P. (2011). Intra-urban societal vulnerability to extreme heat: The role of heat exposure and the built environment, socioeconomics, and neighborhood stability. *Health & Place*, *17*(2), 498–507. https://doi.org/10.1016/j.healthplace.2010.12.005

United States Diabetes Surveillance System. (2021). [CSV Data File]. Centers for Disease Control and Prevention. Retrieved from https://gis.cdc.gov/grasp/diabetes/diabetesatlas-surveillance.html

Whitman, S., Good, G., Donoghue, E. R., Benbow, N., Shou, W., & Mou, S. (1997). Mortality in Chicago attributed to the July 1995 heat wave. *American Journal of Public Health*, *87*(9), 1515–1518. https://doi.org/10.2105/ajph.87.9.1515

Wilson, B. (2020). Urban heat management and the legacy of redlining. *Journal of the American Planning Association*, *86*(4), 443–457. https://doi.org/10.1080/01944363.2020.1759127

Wold, S., Esbensen, K., & Geladi, P. (1987). Principal component analysis. *Chemometrics and Intelligent Laboratory Systems*, *2*(1), 37–52. https://doi.org/10.1016/0169-7439(87)80084-9

Wolf, T., & McGregor, G. (2013). The development of a heat wave vulnerability index for London, United Kingdom. *Weather and Climate Extremes*, *1*, 59–68. https://doi.org/10.1016/j.wace.2013.07.004

World Health Organization. (2021). *Climate change and health: Vulnerability and adaptation assessment*. W. H. Organization. Retrieved from https://www.who.int/publications/i/item/9789240036383

Xu, Y., Dadvand, P., Barrera-Gómez, J., Sartini, C., Marí-Dell'Olmo, M., Borrell, C., et al. (2013). Differences on the effect of heat waves on mortality by sociodemographic and urban landscape characteristics. *Journal of Epidemiology & Community Health*, *67*(6), 519–525. https://doi.org/10.1136/jech-2012-201899

Xu, Z., Fitzgerald, G., Guo, Y., Jalaludin, B., & Tong, S. (2016). Impact of heatwave on mortality under different heatwave definitions: A systematic review and meta-analysis. *Environment International*, *89–90*, 193–203. https://doi.org/10.1016/j.envint.2016.02.007

Yin, Q., Wang, J., Ren, Z., Li, J., & Guo, Y. (2019). Mapping the increased minimum mortality temperatures in the context of global climate change. *Nature Communications*, *10*(1), 4640. https://doi.org/10.1038/s41467-019-12663-y

Zanobetti, A., & Schwartz, J. (2008). Temperature and mortality in nine US cities. *Epidemiology*, *19*(4), 563–570. https://doi.org/10.1097/EDE.0b013e31816d652d

Zanobetti, A., O'Neill, M. S., Gronlund, C. J., & Schwartz, J. D. (2013). Susceptibility to mortality in weather extremes: Effect modification by personal and small-area characteristics. *Epidemiology*, *24*(6), 809–819. https://doi.org/10.1097/01.ede.0000434432.06765.91

Zhai, P., Pirani, A., Connors, S., Péan, C., Berger, S., Caud, N., et al. (2021). IPCC 2021: Climate change 2021: The physical science basis. In *Contribution of working group I to the sixth assessment report of the intergovernmental panel on climate change*. Cambridge University Press.